LA-6127-MS
Informal Report

C.3

UC-79p
Reporting Date: October 1975
Issued: November 1975

Effects of Neutron Streaming and Geometric Models on Molten Fuel Recriticality Accidents

by

Thomas P. McLaughlin

los alamos
scientific laboratory
of the University of California
LOS ALAMOS, NEW MEXICO 87545

An Affirmative Action/Equal Opportunity Employer

UNITED STATES
ENERGY RESEARCH AND DEVELOPMENT ADMINISTRATION
CONTRACT W-7405-ENG. 36

In the interest of prompt distribution, this report was not edited by the Technical Information staff.

Work supported by the U.S. Energy Research and Development Administration's Division of Reactor Research and Development.

Printed in the United States of America. Available from
National Technical Information Service
U S Department of Commerce
5285 Port Royal Road
Springfield, VA 22151
Price: Printed Copy $4.00 Microfiche $2.25

EFFECTS OF NEUTRON STREAMING AND GEOMETRIC MODELS ON MOLTEN FUEL RECRITICALITY ACCIDENTS

by

Thomas P. McLaughlin

ABSTRACT

A postulated fast reactor accident which has been extant for many years is a recriticality following partial or complete core melting. Independently of the cause or probability of such a situation, certain cases can be defined and some facets of the dynamic history of these cases can be described with more than enough accuracy for safety considerations. Calculations were made with the PAD code for systems with 10 vol% voids and varying reactivity insertion rates. Additionally, two distinct geometric and equation of state models were investigated in conjunction with a model which accounted for possible neutron streaming reactivity effects. Significant results include fission and kinetic energy, temperatures and pressures.

I. INTRODUCTION

This report continues the study of criticality energetics should a mass of fast reactor fuel become molten, reasonably homogeneous, and have imposed upon it reactivity added at a high, constant rate. The situation is further specialized to represent the case of a mildly boiling liquid. The neutronics model in the PAD code accounted for possible reactivity changes should bubbles collapse during a rapid power (and liquid temperature) rise; and two hydrodynamics models, treating voids both explicitly and implicitly, were included in the study.

Previous progress reports and publications on this subject have reported energy releases from similar, postulated recriticality events.[1,2,3] All of the prior studies, however, employed an implicit void treatment and did not consider possible reactivity feedback resulting from changes in the neutron mean chord length. A recent progress report analyzed the neutronics and reactivity worth of voids in fissile systems.[4] This reactivity is associated with the streaming of neutrons through randomly distributed bubbles or voids and is commonly known as the Behrens effect.[5] This report describes a first attempt to combine the reactivity feedback that is possible from the collapse of bubbles with the PAD code, employing an explicit void treatment. Continuing examination of some conservatisms and model assumptions may be necessary for a realistic evaluation of this hypothetical scenario.

Prior transport calculations quantified the Behrens effect for systems characterized by fuel with a k_∞ of 1.33.[4] This analysis has been extended to include fuel compositions with k_∞ = 1.50 and k_∞ = 2.00. As before, these results are compared with the theoretical work reported by Nicholson.[6] A neutronics model has been incorporated into the PAD analyses which calculates the

(regionwise) reactivity feedback associated with changes in the void content at each time step. This model also includes a spatial reactivity weighting function.

The hydrodynamics models were idealized to unreflected spheres of fuel of radii 29, 44, and 53 cm, corresponding to fuels with k_∞ = 2.0, 1.5, and 1.33, respectively. An average initial void content of 10 vol% was employed in all calculations. Parameter variations were performed for: reactivity insertion rate; streaming reactivity feedback (magnitude and spatial weighting function); geometric model (homogeneous and layered); void size. Significant results include fission and kinetic energy releases as well as reactivities, temperatures, and pressures.

In order that the postulated scenario and underlying models and assumptions be clear, they are: (1) an incident occurs which leads to fuel and clad melting, (2) a container is afforded either by fuel and clad freezing in the lower reflector regions or by other structures below the core, (3) more fuel melts and is contained in this "bucket"; (4) the retained fuel boils, either because of decay heat or from fission heating, (5) something (unspecified) causes a severe reactivity ramp and power excursion with a subsequent sharp temperature rise, and (6) the rapid temperature rise causes the liquid fuel to expand and collapse the vapor bubbles. This collapse produces a decrease in the neutron mean chord length and a positive reactivity feedback - in addition to the impressed ramp.

II. STREAMING REACTIVITY ANALYSIS

The magnitude and consequences of reactivity changes accompanying the partial or complete collapse of a distribution of gas or vapor bubbles has been the subject of recent reports.[4,6,7] This bubble collapse is postulated to occur as a result of expansion (heating) of the surrounding material during a power transient. However, it should be emphasized that accompanying the expanding liquid are three reactivity effects, all interdependent:

- Mass-importance
- Mean chord length (streaming)
- Self-multiplication.

The first feedback effect is a result of material motion in a neutron importance gradient (i.e., reactivity worth gradient). This effect will, in fissioning systems with positive buckling, likely be negative, of similar or larger magnitude than the second effect and act on the same time scale. The third effect is always small and negative over a reasonable range of liquid state density changes. However, in the limit of arrays of fuel units which are themselves nearly critical, self-multiplication is the dominant effect. Prior analyses of the second reactivity feedback effect alone and the second and third effects in combination have been referenced. The latter are extended in the following section.

A. Magnitude

A qualitative picture (Fig. 1) of the change in the state of criticality of a

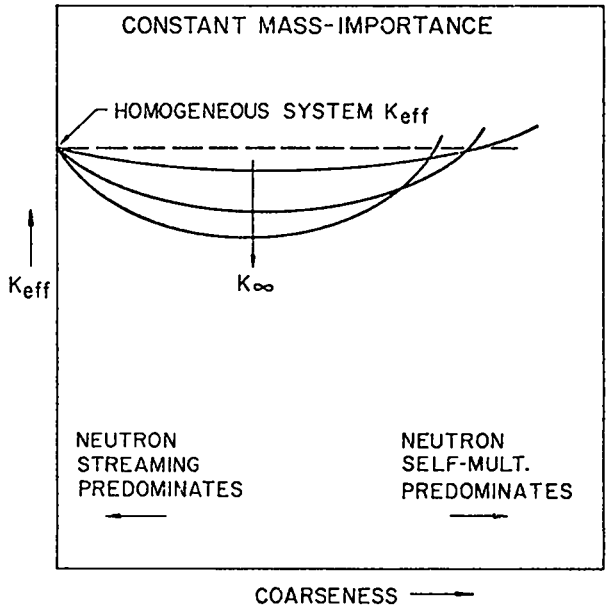

Fig. 1. State of criticality vs system coarseness.

total mass of fuel within a fixed outer boundary as one changes the system from a homogeneous distribution of fuel to one with increasing coarseness may be drawn based on the two limiting reactivity effects: coarseness very small, Behrens' effect predominates; coarseness very large, self-multiplication as typified by ORNL experiments predominates.[9,10,11,12] Changes in the mass-importance are assumed zero in this qualitative picture.

Although in a molten fuel situation one would expect to be in the regime where the Behrens effect predominates over self-multiplication, the calculated net reactivity effect during a power transient is very model-dependent since mass-importance changes will be significant.

Since the reactivity effects in question may be adequately described by a one energy group representation, a two-dimensional transport theory analysis was possible without excessive computing costs. In order to isolate this reactivity feedback, it was necessary to employ a geometry which enabled mass motion at essentially constant importance.

As previously reported,[4,7] an adequate calculational tool is available in the form of the TWOTRAN SPHERE computer program.[8] That this S_N code accurately calculates neutron streaming for the chosen model has been verified via Monte Carlo analysis.[7] This code employs S_N transport theory in r,θ spherical geometry; r being distance from the origin and θ being an angle measured from the pole with $0 < \theta_{max} \leq \pi$. Two-π symmetry is assumed around the pole. This geometry can best be visualized by inspection of Fig. 2.

This geometry has the advantage of r,θ cylindrical geometry in that mass can be lumped/distributed within an r to r + Δr shell, essentially eliminating mass-importance effects. In addition it possesses one significant advantage: due to the curvature of the mesh volumes in spherical geometry, neutron streaming paths are

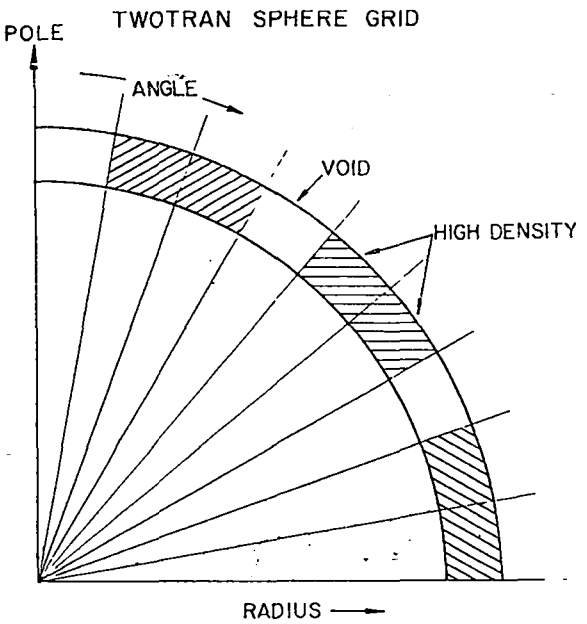

Fig. 2. Example of TWOTRAN SPHERE mesh. Revolution of this plane through 2 radians, about the pole, yields the hemispherical geometry used in the calculations. Note that most volume elements (mesh cells) are somewhat toroidal shaped. Those elements bounding the Pole are frustums of cones. Those elements bounding the origin (r= 0) are spherical sectors.

more well defined and an estimate of an average "bubble" size is more realistic and accurate than for r,θ cylindrical geometry. From a different viewpoint the spherical geometry is also desirable; it enables comparisons with the theoretical results in Ref. 6.

Prior analyses of the streaming effect with the TWOTRAN SPHERE code were made for only one system size, a 53-cm sphere.[4] The infinite medium multiplication factor for the fuel in that study was $k_\infty = 1.33$. Those results, together with results for 44-cm ($k_\infty = 1.5$) and 29-cm ($k_\infty = 2.0$) spheres and with void contents of 10 and 33 vol% are presented in Figs. 3 through 8.

The only parameter in this work which is subjective is the characterization of the average "bubble" size in the r,θ spherical geometry. The three coarse meshes (r x θ = 10 x 9; 20 x 18; 40 x 36)

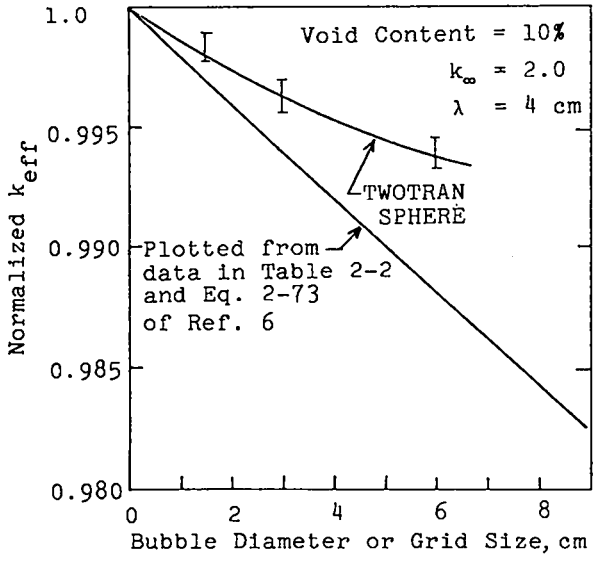

Fig. 3. State of criticality vs system coarseness at constant mass-importance.

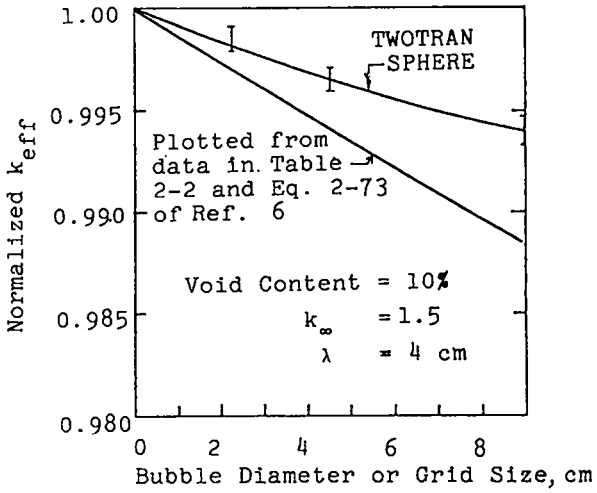

Fig. 5. State of criticality vs system coarseness at constant mass-importance.

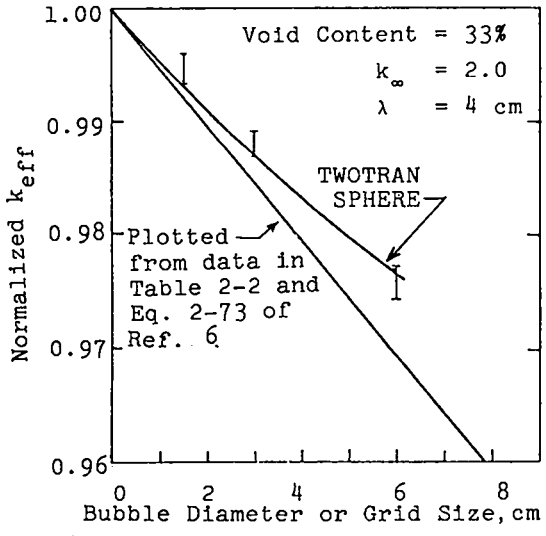

Fig. 4. State of criticality vs system coarseness at constant mass-importance.

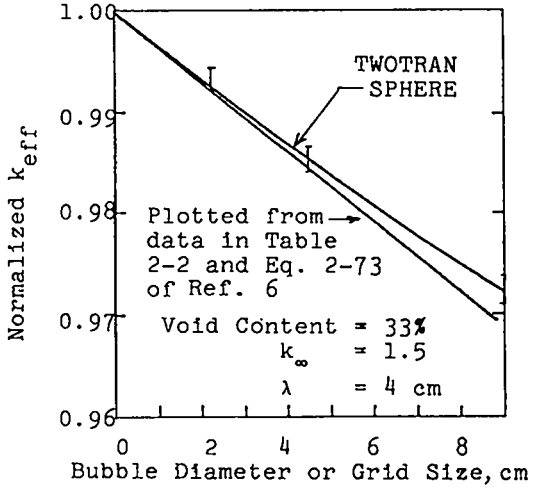

Fig. 6. State of criticality vs system coarseness at constant mass-importance.

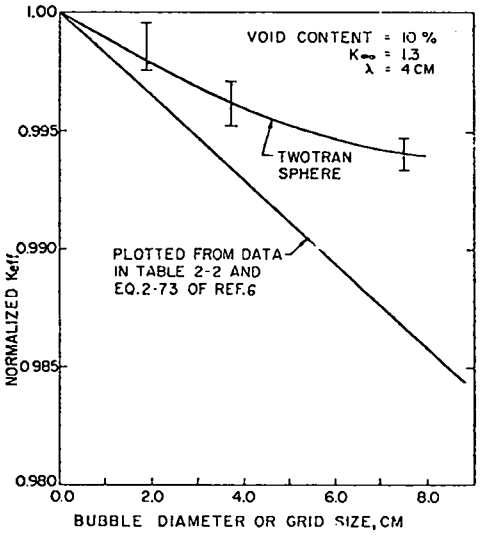

Fig. 7. State of criticality vs system coarseness at constant mass-importance.

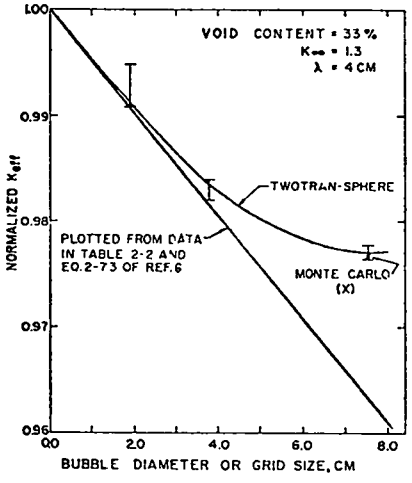

Fig. 8. State of criticality vs system coarseness at constant mass-importance.

employed in this study correspond to the three data points shown on each figure. Since each mesh cell in this geometry has a different volume, i.e., a different average chord length for neutrons, no attempt was made to calculate an exact average "bubble" size. The error bars represent estimated uncertainties due to S_N, fine mesh size and convergence effects. The reactivity shown in these figures is the maximum which would be added to the system if all the voids were filled with the expanding liquid. If, during a postulated excursion, only partial void collapse occurred then only a fraction of the reactivity represented in these plots would be added as positive feedback.

The results in these figures, however subjective, do indicate that, in the absence of mass-importance effects and for credible bubble sizes and void fractions, the Behrens effect dominates other reactivity effects and is at least approximately correct as calculated in Ref. 6. It is significant that all curves resulting from this work show the predicted shape as shown in Fig. 1.

In order to relate these different-size systems to actual LMFBR fuels, transport calculations employing the 16 group Hansen and Roach cross-section set and the DTF code were made for the feed fuel composition planned for the inner and outer core zones of both FFTF and CRBRP.[13] The results of this analysis are presented in Table I. It is evident from these results that: (1) the total mean free path, λ, of 4 cm which was used in the prior and current one-group TWOTRAN SPHERE and PAD analyses is adequate and (2) the studies for the 29-cm sphere are most applicable for these two fast reactors. Although k_∞ is independent of any void content, homogenized or discrete, the critical radius is strongly dependent thereon. The critical radii in Table I are based on 90% dense fuel (10 vol% voids).

TABLE I

FFTF AND CRBRP FEED FUEL CHARACTERISTICS

Fuel	k_∞	Critical Radius cm
FFTF Inner	1.82	33.3
FFTF Outer	2.10	26.0
CRBRP Inner	1.73	35.7
CRBRP Outer	2.02	27.5

B. Spatial Weighting Function

The reactivity change accompanying partial or complete bubble collapse is due to changes in neutron leakage from the system. As such it is proper to weight the reactivity feedback spatially with a neutron current function. Further since a bare, one-group system is self-adjoint ($J = J^+$), a weighting function which is appropriate for the chosen model is the current squared, $J^2(r)$.

Due to the direct availability of fluxes (but not currents) from the DTF k-calculator which is imbedded in the PAD code, it was decided to first consider the applicability of a flux-based weighting function. A relationship which was considered (and actually employed in a few calculations, for sensitivity studies involving the weighting function) is the function:

$$W(r) = 1-\phi^n(r). \qquad (1)$$

This functional representation, with n = 0 and 1, is in fact what was employed in the studies reported by Nicholson.[6] Since the geometry utilized in this study was spherical, it was possibly to evaluate the J^2 function directly, prior to any PAD calculations. The theoretical form for the neutron flux in a bare, homogeneous, one-group sphere is:

$$\phi(r) \sim A \frac{\sin\pi r/R_e}{r}. \qquad (2)$$

The current then has the form:

$$J(r) \sim \frac{d\phi}{dr} \sim A \frac{(\pi r/R_e)\cos\pi r/R_e - \sin\pi r/R_e}{r^2}. \qquad (3)$$

This function, normalized to unit amplitude, is shown in Fig. 9 for a 53-cm bare sphere and an extrapolated radius, R_e = 55.8 cm. The normalized weighting function, $J^2(r)$, is plotted in Fig. 10. For

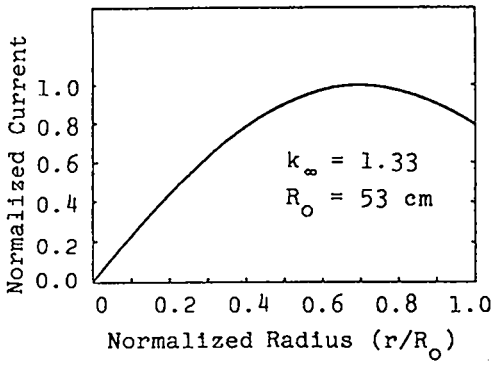

Fig. 9. Neutron current for a bare, one-group sphere.

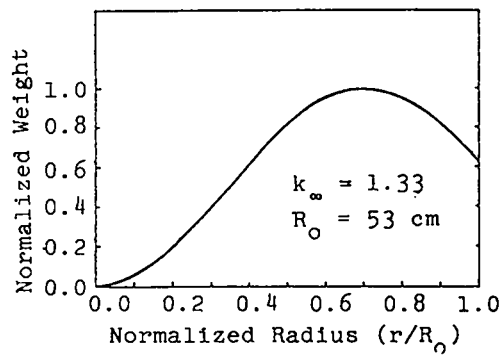

Fig. 10. Current squared weighting function for a bare, one-group sphere.

44-and 29-cm bare spheres the current and current squared functions are insignificantly different from Figs. 9 and 10 when plotted on this normalized radius scale. Thus the regionwise weighting coefficients for all three spheres (29-, 44-, 53-cm radius) were based on Fig. 10. An exception to this was the initial investigation of flux based weighting functions which are described below.

A general observation from Fig. 11 is that none of the flux weighting functions are close approximations to the current squared, for all spatial locations. Although it appears that agreement is better for larger exponents (n ~ 4), the degree of accuracy of any flux weighting of this form would be problem-dependent. For example, a mild excursion may result in void closure predominantly in the inner regions, while for a more energetic excursion (larger

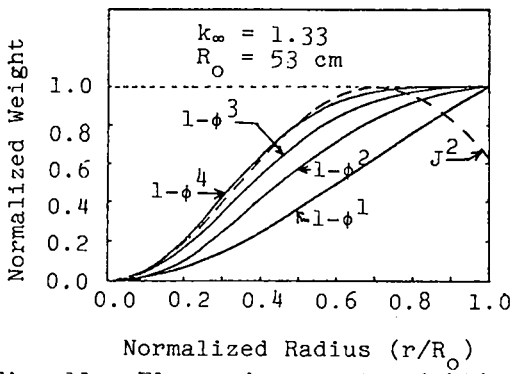

Fig. 11. Flux and current weighting functions for a bare, one-group sphere.

temperature rise) void closure may be complete over the entire fissioning system. To avoid these uncertainties it was decided to modify the PAD code to accept mass point, but otherwise arbitrary, weighting coefficients, i.e., from Fig. 10.

C. PAD Code Modification

Reactivity feedback due to changes in neutron streaming (migration area changes) was treated implicitly in the PAD calculations. The degree of bubble collapse associated with each core zone was directly related to the temperature rise in the zone. This is similar to the treatment of this effect used in the VENUS analyses reported by Nicholson.[6]

The streaming reactivity feedback was then calculated at each time step in the PAD calculation according to the formulas:

$$\Delta k_i(t) = \frac{\Delta K_B \times J_i^2 V_i [T_i - T_i^o / T_i^* - T_i^o]}{\sum_i J_i^2 V_i} \qquad (4)$$

and

$$\Delta K(t) = \sum_i \Delta k_i(t) \qquad (5)$$

where

ΔK_B = total reactivity change associated with complete bubble collapse, from Figs. 3-8.

i = zone index

J_i^2 = zone reactivity weighting coefficient, from Fig. 10

V_i = zone volume at time t

T_i = zone temperature at time t

T_i^o = zone initial temperature

T_i^* = zone temperature at which the initial void content is entirely filled by liquid fuel expansion.

If the zone temperature exceeded T^*, then Δk_i was held constant at the value corresponding to T^*.

III. GEOMETRIC AND EQUATION OF STATE MODELS

The postulated excursion is examined by the application of two different geometric and equation of state models. Additionally the conservatisms and advantages or disadvantages of each model are discussed, particularly in the context of the bubble collapse reactivity feedback. These models are identified by the labels homogeneous and layered which characterize the fuel spatial distributions. Associated with these respective geometric models are "threshold" and "nonthreshold" equation of state treatments, both of which are variations of the basic PAD EOS model for the condensed phase.

The calculational geometry was one-dimensional, spherical with each region (mass point) representing a spherical shell. The neutronics for determining the state of criticality, power profile, and the displacement reactivity feedback was based on a one energy group representation. Initial conditions and other assumptions employed in the PAD calculations are summarized below.

- Initial power = 1.0 MW
- Initial temperature = 3123 K, this is the PAD melt temperature for UO_2, which is assumed to be liquid.
- Initial density (fully dense) = 8.7 g/cm^3
- Initial state of criticality = prompt critical

- Prompt neutron lifetime = 67 ns
- No delayed neutrons
- All physical properties data correspond to pure UO_2
- System averaged void content = 10 vol%
- Doppler constant = -0.002
- Total neutron mean free path = 4.0 cm.

These model specifications are identically those employed in studies reported previously.[1,2,3] The S_N quadrature and one-group cross sections specified for the PAD analyses were the same as for the TWOTRAN SPHERE calculations.

A. PAD EOS Model for UO_2

Thy hydrodynamic (working) pressure for UO_2, and for many other materials in the PAD code, is discretized into condensed phase (solid and liquid) and vapor phase functions. The condensed state function has the form:

$$P_s = \alpha B\ (T-T_o) + B/\rho\ (\rho-\rho_o) \qquad (6)$$

where

P_s = condensed phase pressure, dynes/cm^2

α = volume coefficient of expansion, K^{-1}

B = bulk modulus, dynes/cm^2

T = temperature, K

ρ = density, g/cm^3.

In addition to this a vapor phase pressure is allowed, whose temperature dependence is required to follow the saturation line,

$$P_e = P_o\ e^{-L/RT}, \qquad (7)$$

where L is the heat of vaporization, R is the universal gas constant ($\sim$ 2 cal/g-mole) and P_o is a constant determined by requiring that (7) satisfy critical point data. For UO_2, the data used in the PAD code are:

- Heat of vaporization = 1866 J/g
- Critical Point: P = 1974 atm, T = 7500 K.

With this information Eq.(7) can be solved for the 1-atmosphere boiling point, resulting in T_B = 3650 K. Both the heat of vaporization and boiling point compare favorably to recently reported "recommended values" (1925 J/g; 3693 K, Ref. 14).

For determining the vapor fraction a perfect gas equation is assumed:

$$P_v = f\ R\ \rho\ T \qquad (8)$$

where P_v is equated to P_e from (7), f is the mass fraction vaporized, R is from (7), ρ is the total fuel density (vapor + liquid), and T is temperature. Although the total (hydrodynamic) pressure was set equal to the sum of the condensed and vapor state pressures in this study, condensed phase pressures were the major disassembly mechanism for all cases presented in the RESULTS section.

B. Homogeneous Geometry Model

In this model the material density is spatially uniform. The initial void content is accounted for by reducing the material density according to the formula.

$$\rho = \rho_o\ (1 - \bar{V}), \qquad (9)$$

where ρ_o = normal material density at temperature T_o

$\bar{V}$ = system initial void fraction

ρ = reduced material density at temperature T_o.

The liquid phase equation of state, (6), exhibits a "threshold" in this model. Since the second term in this equation is negative, positive pressures do not act until the temperature in a zone has reached a value such that

$$\alpha B(T-T_o) > B/\rho\ (\rho-\rho_o). \qquad (10)$$

Initial zone temperatures, T, are set equal to T_o, so that the first term, $\alpha B(T-T_o)$, is

identically zero at the start of a calculation. A further restriction in this model is that negative pressures (tensile strengths) are not allowed, i.e., if the calculated $P_S < 0$, then P_S is set equal to zero.

This is obviously a conservative model. Prior to temperatures reaching the threshold, the only reactivity quenching mechanisms are those resulting from vapor pressures and the Doppler effect.

C. Layered Geometry Model

This model consists of a series of concentric shells, as does the homogeneous model, but with an appropriate number of these shells void. Thus, in this geometry voids are accounted for explicitly albeit as spherical shells. The motivation for the development of this model was to find a representation which was less conservative (more realistic) than the homogeneous model. The original employment of this model was directed at the analysis of a postulated EBR-II core collapse accident.[15]

This model has been applied to the problem at hand by placing the 10% void volume in the form of concentric shells either 1 or 3 cm thick to simulate bubbles of 1 and 3 cm diameter respectively. These voided shells are separated by shells of full density material. The dynamics of the PAD code allows motion both inward and outward as demanded by the pressure gradients. This effect leads to numerical difficulties as a void shell approaches zero volume. To counter this problem, fuel at 5% of the normal density was specified for these regions.

The condensed phase equation of state, (6), for the fully dense zones has $\rho = \rho_o$ and $T = T_o$ at the start of the PAD calculations. Therefore for these zones there is no "threshold"; pressures rise as soon as temperatures increase. Expansions follow which lead directly to material motion feedback as calculated by explicit transport (DTF) analysis.

D. Model Conservatisms

Both of the models employed have different advantages, disadvantages, and conservatisms. Although a liquid containing bubbles is not homogeneous, communication paths from center to edge would exist, allowing transmission of pressure waves. The velocity of the pressure waves would be reduced relative to a fully dense system (e.g., the Godiva reactor). The degree of reduction is dependent on the bubble size, distribution, and system void (bubble) content. Neither the homogeneous (threshold) model nor the layered model permits this pressure wave propagation; for this reason both are conservative.

The spherical geometry considered in this study is nonconservative with respect to critical mass but probably conservative with respect to the calculated kinetic energy. That is, a dish-shaped critical mass (for example, as may be postulated to occur in the core support structure) would contain more mass than a critical sphere of the same fissile material. However, the characteristic dimension for pressure wave propagation (e.g., radius of a sphere; half-thickness of a slab) is larger for the sphere. Thus expansion feedback effects will be felt sooner in nonspherical geometry.

Prior studies have indicated that reflected spheres yield lower energy releases, pressures, and temperatures than bare spheres.[1,3] This is most probably due to the smaller critical mass for the same fuel material, in the reflected case. Additionally, since the streaming reactivity effect is directly related to system leakage, it follows that for reflected systems any bubble collapse reactivity feedback calculated for a bare sphere is conservative when applied to the reflected sphere. If an LMFBR core meltdown were to occur and, further, a molten fuel recriticality were postulated, then there would necessarily be reflection over $\sim$ one-half of the surface of the contained molten fuel. Thus from

both expansion and streaming reactivity feedback considerations any realistic geometry is conservative relative to the idealized, bare geometries analyzed herein.

The threshold model has been widely applied to postulated molten fuel recriticality studies because it is believed to be conservative and allow the calculation of bounding values (energy releases, temperatures, pressures, etc.). Certainly if one couples an additive, positive reactivity feedback (to model possible streaming effects) to a threshold EOS model, then there is a very high degree of conservatism in the analysis, at least from these considerations.

The layered model was developed to provide a description somewhat less conservative than the threshold model but which still allowed for inhomogeneities of an arbitrary nature to be modeled. Reactivity changes caused by expansion of the fuel into the voided shells are calculated correctly (except that the one-dimensional model does not inherently account for the bubble collapse effect, which was then handled separately), and the outermost surface is allowed to expand. But, as noted above, a pressure wave generated in the center is not propagated outward in a realistic manner. All factors considered, this model is judged to be conservative and, for the case at hand, a better approximation to the hypothetical model than the homogeneous (threshold) model.

IV. RESULTS

Parameter variations in the present study included reactivity insertion rate, geometric and equation of state models and streaming reactivity feedback (magnitude and spatial weighting). The void fraction and Doppler coefficient were held constant at 0.10 and -0.002, respectively. Studies varying these latter two parameters, but without consideration of streaming reactivity effects, have been reported.[3]

Power, fission energy, and kinetic energy histories from a PAD calculation for one of the cases are shown in Fig. 12. The corresponding net and individual reactivity traces are given in Fig. 13. These results are qualitatively representative of all cases studied, including the above referenced work on multizone systems (radially varying void fractions). This consistency is due to a common, dominant material motion mechanism, namely, liquid state pressures.

Since the system temperature rise follows the fission energy deposition history, it is apparent from Fig. 12 that temperatures begin to rise substantially at about 1.8 ms and maximum values are reached by 2.4 ms. This temperature-time dependence explains the Doppler and streaming reactivity feedback traces on Fig. 13. For this particular case it is noteworthy that although the streaming reactivity feedback model resulted in the insertion of almost twice the reactivity removed by Doppler feedback, this did not aggravate the excursion greatly. Material motion feedback,

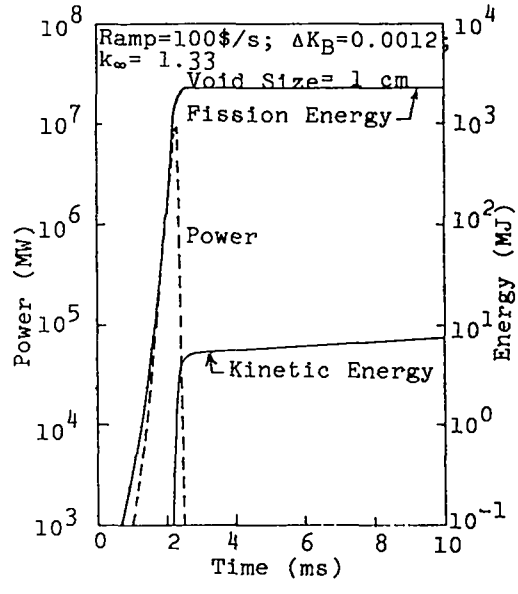

Fig. 12. Power and energy histories for a typical case.

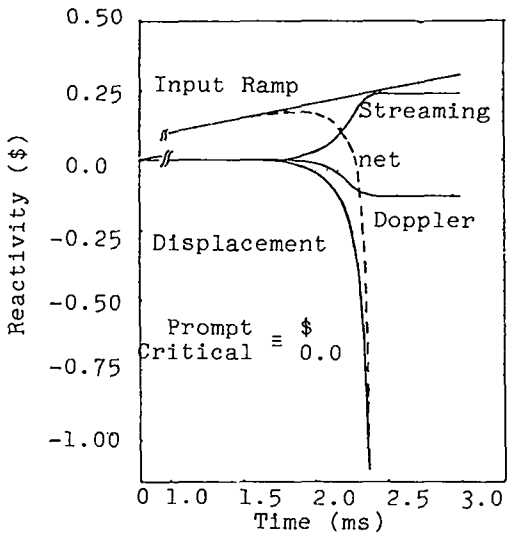

Fig. 13. Input, feedback and net reactivity histories.

which occurred on the same time scale as the former, was dominant.

The high solid state pressures which precipitate the material motion also provide the explanation for the initial, steep rise in the kinetic energy trace. After the power burst is complete (∿ 2.4 ms), expansion of the dense regions into the voided regions and expansion at the outer boundary quickly relieve the liquid phase pressures. The subsequent slow rise in the kinetic energy results from the generation of fuel vapor pressures.

The parametric survey of cases studied is presented in Tables II, III and IV for critical spheres of 29.0, 44.0 and 53.0 cm respectively. There are several points to be noted from these tables.

- Energy releases (fission and kinetic) are strongly dependent on both the degree of model heterogeneity (i.e., homogeneous; 1.0 cm shells; 3.0 cm shells) and the magnitude of the streaming reactivity feedback.
- Energy releases increase monotonically with the system critical mass.
- Results for homogeneous model calculations without streaming feedback are similar to those results which employed the layered model with a best estimate ΔK_B.
- For very reactive fuel ($k_\infty \sim 2.0$), reactivity insertion rates in excess of \$1000/s would be necessary for a destructive excursion.
- The streaming reactivity weighting function plays a relatively unimportant role, at least when employed

TABLE II

PAD RESULTS FOR 29-CM SPHERE

$K_\infty = 2.0$ Void Fraction ≈ 0.10

Void Size cm	ΔK_B	Fission Energy MJ	Kinetic Energy MJ	Core Average Temperature, K	Core Average Pressure, atm	Max. Power MW	Max. Alpha s^{-1}
			50 \$/s				
1.0	.0025	16	∿ 0	3160	≈ 0	1.1 + 4	2.2 + 3
			100 \$/s				
H	0.0	300	0.4	3820	1.8	1.1 + 6	6.5 + 3
1.0	0.0	70	∿ 0	3280	≈ 0	1.3 + 5	5.5 + 3
1.0	.0025	120	∿ 0	3380	≈ 0	2.5 + 5	5.7 + 3
1.0	.0050	320	1.0	3800	5.0	1.1 + 6	6.0 + 3
			300 \$/s				
1.0	.0025	330	1.0	3810	4.5	1.5 + 6	1.3 + 4
			1000 \$/s				
1.0	.0025	566	3.1	4230	11.2	7.3 + 6	2.7 + 4

TABLE III

PAD RESULTS FOR 44-CM SPHERE

K_∞ = 1.50 Void Fraction ≈ 0.10

Void Size CM	ΔK_B	Fission Energy MJ	Kinetic Energy MJ	Core Average Temperature, K	Core Average Pressure, atm	Max. Power MW	Max. α s^{-1}
			50 $/s				
1.0	.0018	600	≈ 0	3490	1.0	9.4+5	2.3+2
			100 $/s				
H	0.0	1110	3.3	3860	2.4	5.6+6	8.1+3
1.0	0.0	610	≈ 0	3490	1.1	1.6+6	7.3+3
1.0	.0018	1080	2.0	3770	4.6	3.1+6	7.8+3
1.0	.0036	1630	10.4	4060	7.7	1.1+7	8.3+3
			300 $/s				
1.0	.0018	1530	8.3	3990	6.5	9.8+6	1.5+1
			1000 $/s				
1.0	.0018	2760	74.0	4690	30	3.9+7	3.0+1

TABLE IV

PAD RESULTS FOR 53 CM SPHERE

K_∞ = 1.33 Void Fraction ≈ 0.10

Void Size cm	ΔK_B	Fission Energy MJ	Kinetic Energy MJ	Core Average Temperature, K	Core Average Pressure, atm	Max. Power MW	Max. α s^{-1}
			50 $/s				
H	0.0	1720	3.7	3780	2.7	5.7 +6	5.8 +3
1.0	.0012	1120	~0	3510	1.0	1.9 +6	5.3 +3
3.0	.0036	610	~0	3340	0.4	1.0 +6	5.1 +3
			100 $/s				
H	0.0	2170	11.7	3940	5.0	1.1 +7	9.0 +3
H	.0012	3200	50.0	4320	13.9	2.5 +7	1.4 +4
H	.0024	5034	180.0	4930	41.0	6.0 +7	2.4 +4
H	.0036	8720	610.0	6000	137.0	1.4 +8	3.6 +4
1.0	.0012	2290	8.6	3860	5.1	9.3 +6	5.6 +3
1.0	.0024	3210	35.0	4150	11.6	2.1 +7	1.0 +4
1.0	.0036	4090	130.0	4660	33.0	5.1 +7	2.0 +4
1.0	.0012[a]	2290	8.7	3860	5.3	9.4 +6	8.5 +3
1.0	.0012[b]	2160	7.5	3820	6.0	8.0 +6	8.3 +3
1.0	.0012[c]	2200	7.9	3830	5.8	8.4 +6	8.4 +3
1.0	.0012[d]	2230	8.1	3840	5.7	8.6 +6	8.5 +3
1.0	.0012[e]	2290	8.6	3860	5.1	9.3 +6	8.5 +3
3.0	.0036	940	0.3	3450	1.1	2.6 +6	8.0 +3
			300 $/s				
H	0.0	3480	62.0	4290	16.6	3.1 +7	1.7 +4
1.0	.0012	3430	48.0	4240	15.0	2.8 +7	1.7 +4
3.0	.0036	1900	6.6	3760	6.1	1.1 +7	1.5 +4
			1000 $/s				
H	0.0	7120	410.0	5560	93	1.1 +8	3.3 +4
1.0	.0012	7040	340.0	5290	75	1.1 +8	3.2 +4
3.0	.0036	3520	55.0	4330	17.7	6.1 +7	3.2 +4

[a] Flux weighting exponent ($W = 1-\phi^n$): a(n=0); b(n=1); c(n=2); d(n=3); e(n=4)

in conjunction with the layered model.

Due to the diversity of the parameter variations present in these tables, only a part thereof is suitable for graphical presentation. For layered model cases with 1.0-cm-thick voided shells and the best estimate ΔK_B, fission and kinetic energy releases are shown in Figs. 14 and 15, respectively.

V. CONCLUSIONS

Two highly idealized models of a hypothetical molten fuel recriticality accident have been developed and applied, via the PAD code, to determine energy releases and other significant parameters which characterize the postulated excursions. Within the framework of the stated models and assumptions it is concluded that:

- A negligible explosive potential exists for these hypothetical situations unless there exist mechanisms (with sufficient probability) for inserting reactivity at extremely high rates.

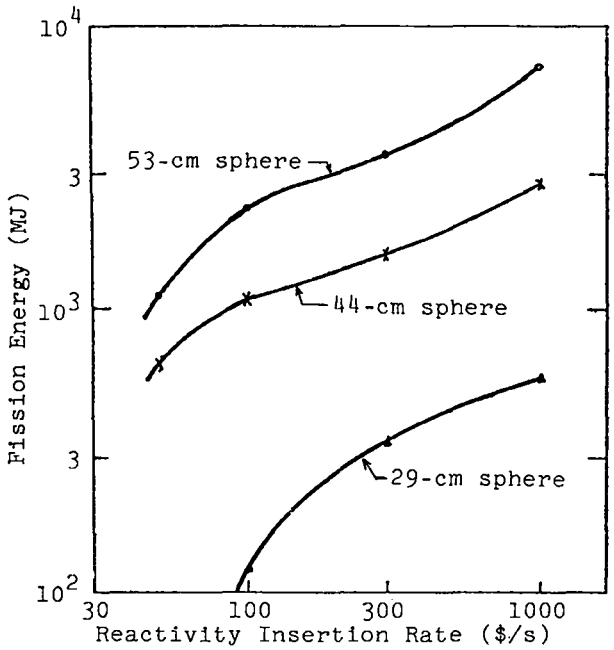

Fig. 14. Fission energy deposition for layered geometry models.

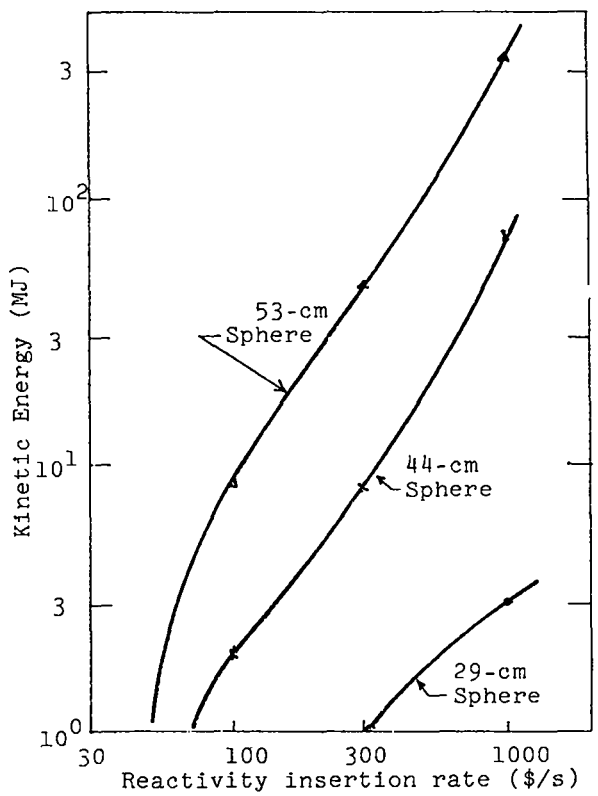

Fig. 15. Kinetic energy (at $V/V_0 = 8$) for layered geometry models.

An attempt has been made to examine the models and assumptions employed in this analysis relative to the degree of conservatism/nonconservatism in each. It is believed that the coupling of a streaming reactivity feedback formalism to a homogeneous (threshold) geometric and equation of state model is compounding conservatism to a high degree. The layered model, while still considered quite conservative when the streaming reactivity feedback is added thereto, is believed to be a more realistic model for the postulated scenario.

REFERENCES

1. William R. Stratton, Leon B. Engle, and Donald M. Peterson, "Energy Release from Meltdown Accidents," Trans. Am. Nucl. Soc. 17, 362 (1973).

2. Thomas P. McLaughlin, Donald M. Peterson, and William R. Stratton, "Energy Release from Molten-Fuel Recriticality Accidents," Trans. Am. Nucl. Soc. 18, 198 (1974).

3. Thomas P. McLaughlin, Donald M. Peterson, and William R. Stratton, Pajarito Reactor Safety Program unpublished progress report, September 1974.

4. Thomas P. McLaughlin, Donald M. Peterson and William R. Stratton, Pajarito Reactor Safety Program unpublished progress report, November 1974.

5. D. J. Behrens, "The Effect of Holes in a Reacting Material on the Passage of Neutrons," Proc. Phys. Soc. London, Sec. A, 62, 607-616 (1949).

6. R. B. Nicholson, "Design Bases Accident Studies," ERDA Chicago Operations Office report COO-2286-3 (June 22, 1974).

7. Thomas P. McLaughlin and G. David Turner, "Reactivity Changes due to Bubble Growth or Collapse in Molten Fuel Systems," Trans. Am. Nucl. Soc. 21, 281 (1975).

8. Kaye D. Lathrop and Forrest W. Brinkley, "TWOTRAN SPHERE: A FORTRAN Program to Solve the Multigroup Transport Equation in Two-Dimensional Spherical Geometry," Los Alamos Scientific Laboratory report LA-4567 (November 1970).

9. Joseph T. Thomas, "Critical Three-Dimensional Arrays of U(93.2)-Metal Cylinders," Nucl. Sci. Eng. 52, 350-359 (1973).

10. Joseph T. Thomas, "The Criticality of Cubic Arrays of Fissile Material," Union Carbide Corp. Y-12 Plant report Y-CDC-10 (Nov. 3, 1971).

11. Joseph T. Thomas, "Uranium Metal Criticality, Monte Carlo Calculations and Nuclear Criticality Safety," Union Carbide Corp. Y-12 Plant report Y-CDC-7 (Oct. 5, 1970).

12. Joseph T. Thomas, "Generic Array Criticality, an Analytic Representation of Reflected Arrays of Fissile Units," Union Carbide Corp. Y-12 Plant report Y-CDC-13 (Aug. 1, 1973).

13. Clinch River Breeder Reactor Project, PSAR, 4, Table 4.3-30, (1975).

14. Rajendra Kumar, L. Baker, Jr., and M. G. Chasanov, "Ex-Vessel Consideration in Postaccident Heat Removal," Argonne National Laboratory report ANL/RAS 74-29 (October 1975).

15. William R. Stratton, T. H. Calvin,and Roger B. Lazarus, "Analysis of Prompt Excursions in Simple Systems and Idealized Fast Reactors," Second International Conference on the Peaceful Uses of Atomic Energy, 1958, Volume 12, page 196.

☆ U.S GOVERNMENT PRINTING OFFICE 1975—677-343/57